Local strain energy density for the fracture assessment of polyurethane specimens weakened by notches of different shape

M. Peron, S.M.J. Razavi ,F. Berto, J. Torgersen
Department of Mechanical and Industrial Engineering, Norwegian University of Science and Technology (NTNU), Richard Birkelands vei 2b, 7491, Trondheim, Norway.
mirco.peron@ntnu.no, javad.razavi@ntnu.no, filippo.berto@ntnu.no, jan.torgersen@ntnu.no

L. Marsavina
Department of Mechanics and Strength of Materials, Univeritatea Politehnica Timisoara, Timisoara, Romania
msvina@mec.upt.ro

ABSTRACT. Recent studies on local stress fields in proximity of crack and notch tips have shown that Strain Energy Density (SED), averaged in a circular control volume surrounding the point of stress singularities, represents a reliable engineering approach for assessing the brittle fracture of several brittle materials. It is worthy of notice that the application of SED criterion and the reliability of its results are strictly related to the proper determination of fracture parameters, i.e. the critical value of deformation energy W_c and the radius R_c of the control volume. This work presents an experimental methodology for their determination by means of notched specimens for different polyurethane densities, ranging from 100 to 651 kg/m^3. Then, once obtained these critical parameters, the failure load in different types of notches and cracked specimens under mode I have been predicted. Moreover, for cracked specimens under mixed mode and mode II, the authors propose a personal approach that confirms PUR foams can be treated as brittle materials

KEYWORDS. Strain Energy Density; PUR foams; Tensile fracture; Critical radius; Fracture parameters.

OPEN ACCESS

Citation: Peron, M., Razavi, S.M.J., Berto, F. Torgersen, J., Marsavina, L., Local strain energy density for the fracture assessment of polyurethane specimens weakened by notches of different shape, Frattura ed Integrità Strutturale, 42 (2017) 214-222.

Received: 28.06.2017
Accepted: 31.07.2017
Published: 01.10.2017

INTRODUCTION

In the last years, Polyurethane (PUR) has widely gained interest in industrial applications because of its high versatility. In fact, as other polymers like polyethylene (PE), PUR materials can be manufactured in a wide range of densities, obviously determining different applications. In fact at low densities (30 - 200 kg/m^3), being rigid foams having a close cell cellular structure, they are employed as high-resilience seating, rigid foam insulation panels, microcellular foam seals and gaskets, high durable elastomeric wheels and tires and as automotive suspension bushings [1]. Whereas, at higher

densities (> 200 kg/m[3]) they show a porous solid structure, and they are used for fixtures and gauges, master and copy models, draw die moulds, hard parts for electronic instruments [1]. Their mechanical properties have been extensively investigated in the past, showing a relationship, based on the geometry of cellular structure and the relative density, with solid materials used for manufacturing [2,3], and revealing a crushable behaviour in compression, characterized by the capability to absorb considerable amount of energy due to plateau and densification regions. Finally Marsavina [4] reports that they behave as brittle materials under tensile loading, being characterized by a linear elastic behaviour up to fracture.
It is worth to notice that usually in the industrial applications components are designed with notches or they are affected by manufacturing induced defects, which are widely reported to reduce both tensile and fatigue strength [5-7]. Several criteria have been proposed in literature for facture assessment of cracked and notched components [8-16], but among all a strain energy based (SED) approach has revealed to be the most robust in the assessment of brittle fracture resistance of several materials [17-20]. The criterion states that brittle fracture failures occur when the strain energy density averaged in a circular control volume of radius R_c, which surrounds a crack or notch tip, reaches a critical value W_c dependent on the material. The robustness of this criterion has been proved by several works on different notches geometries and on different loading conditions [21-27]. The main purpose of this work is to evaluate the effectiveness of SED criterion on PUR foams, aiming to experimentally evaluate the main parameters of this method, i.e. R_c and W_c.

MATERIALS

Polyurethane materials of four different densities (100, 145, 300 and 708 kg/m[3]) manufactured by Necumer GmbH – Germany, under commercial designation Necuron 100, 160, 301 and 651, were experimentally investigated. At low densities 100 and 145 kg/m[3] the materials have a rigid closed cellular structure, while the PUR materials of higher densities show a porous solid structure (300 and 708 kg/m[3]). A QUANTA™ FEG 250 SEM was used to investigate the microstructures of the materials at different magnifications. The cell diameter and wall thickness were determined by statistical analysis, together with the density of PUR materials obtained experimentally according with ASTM D1622-08. The elastic properties Young modulus and Poisson ratio were determined by Impulse Excitation Technique (ASTM E-1876-01). Tensile strength was determined on dog bone specimens according with a gage length of 50 mm and a cross section in the calibrated zone with 10 mm width and 4 mm thickness, according to EN ISO 527, and described in the research published by Marsavina et al. [28].

PUR Density	100	145	300	708
Young's modulus [MPa]	30.18±1.75	66.89±1.07	281.39±2.92	1250±15.00
Poisson's ratio [-]	0.285	0.285	0.302	0.302
Tensile strength [MPa]	1.16±0.024	1.87±0.036	3.86±0.092	17.40±0.32
Mode I fracture toughness [MPa m$^{0.5}$]	0.087±0.003	0.131±0.003	0.372±0.014	1.253±0.027
Mode II fracture toughness [MPa m$^{0.5}$]	0.050±0.002	0.079±0.004	0.374±0.013	1.376±0.047

Table 1: Elastic, mechanical and fracture properties of PUR materials, by varying the density.

The mode I and II fracture toughness were determined on asymmetric semi-circular bend (ASCB) specimens. A detailed description of these tests is presented in [29,30]. The experimentally values of elastic, mechanical and fracture toughness properties are presented in Tab. 1.

EXPERIMENTAL INVESTIGATION

Tensile test

Different notched specimens were tested under tensile load. Notched specimens with geometries presented in Fig. 1.a,b,c having lateral V, rounded U and circular holes of different diameters D were tested in tensile. The U notched specimens, with blunt curvature radius (R = 4.25 mm), were tested for each density, respectively holed plates with different diameters were tested only for the highest density (708 kg/m^3), geometries and maximum load presented in Tab. 2. Tests were performed at room temperature, on a Zwick/Roell Z005 testing machine with 5 kN maximum load, using a loading rate of 2 mm/min. Four tests were performed for each notch geometry. The specimens' dimensions and the average maximum load are listed in Tab. 2. The obtained load-displacement curves show a linear behavior without plasticity, the failure occurs suddenly and the behavior is brittle.

Notch Shapes	Geometrical parameters [mm]					PUR Density [kg/m^3]			
						100	145	300	708
	l	W	b	D	R	Average Maximum load F_{max} [N]			
V	100	25	15	-	0.25	146.39	185.92	353.74	1811.43
U	100	25	15	-	2	189.45	262.4	397.71	2109.96
	100	30	14	-	4.25	236.5	329	443.6	2173.4
O	100	25	-	10	-	187.89	267.31	521.5	1960.31

Table 2: Geometrical parameters and average maximum load of notched components.

Notch shape: O	Length l = 100 mm		Width W = 25 mm			
Hole diameter [mm]	10	8	7	6	5	3.5
Average maximum load [N]	1960.31	2197.27	2290.76	2491.03	2544.66	2944.64

Table 3: The average maximum load from testing of specimens with hole on tensile.

Bending of asymmetric semi-circular bend (ASCB)

ASCB specimens with vertical crack were considered, Fig. 1.d. The crack tip was introduced using a razor blade. Different types of applied mixed mode are easily obtained only by changing one of the supports position (S_2) and keeping constant the other support (S_1). The load is applied on the symmetry axis of the specimen using three point bending grips. Stress intensity factors (SIFs) solution for ASCB specimen [31]:

$$K_i = \frac{P_{max}}{2Rt}\sqrt{\pi a}Y_i(a/R, S_1/R, S_2/R) \qquad i = I, II \tag{1}$$

were obtained by finite element analysis (Lazzarin and Filippi, [32] and are plotted for a crack length a = 20 mm, specimen radius R = 40 mm, distance to fixed support S_1 = 30 mm, thickness t = 10 mm, resulting a/R = 0.5, S_1/R = 0.75. It could be observed that changing the distance S_2 from 30 mm to 3 mm, the loading conditions change from pure mode I to dominant mode II conditions. Moreover, using a polynomial interpolation the exact position of left support, leading to pure mode II loading condition, was determined at distance S_2 = 2.66 mm. The recorded load–displacement curves were linear (no significant non-linearity identified) and the fracture occurred suddenly, indicating that the specimens failed in a brittle manner, Fig. 1.e. Tab. 4 presents the average fracture load values F_{max} obtained at each loading configuration for the four considered materials. For all the tested specimens the thickness was equal to 10 mm. The mixed mode ratio was quantified using the mode mixity through the dimensionless parameter M^e, proposed by Ayatollahi and Torabi [33].

	M^e (S_2 [mm])					
Density [Kg/m^3]	1(30)	0.83 (12)	0.651 (8)	0.472 (6)	0.206 (4)	0.004 (2.66)
100	43.8	88.5	91.47	102.55	97.3	92.4
145	67.8	133.5	152.5	158	151.25	148.67
300	190	397.5	535.5	645	601.75	712.3
708	704.3	1340	1680	1910	2133	2130
	Average Fracture Load Value [N]					

Table 4: Average fracture loads values for ASCB specimens.

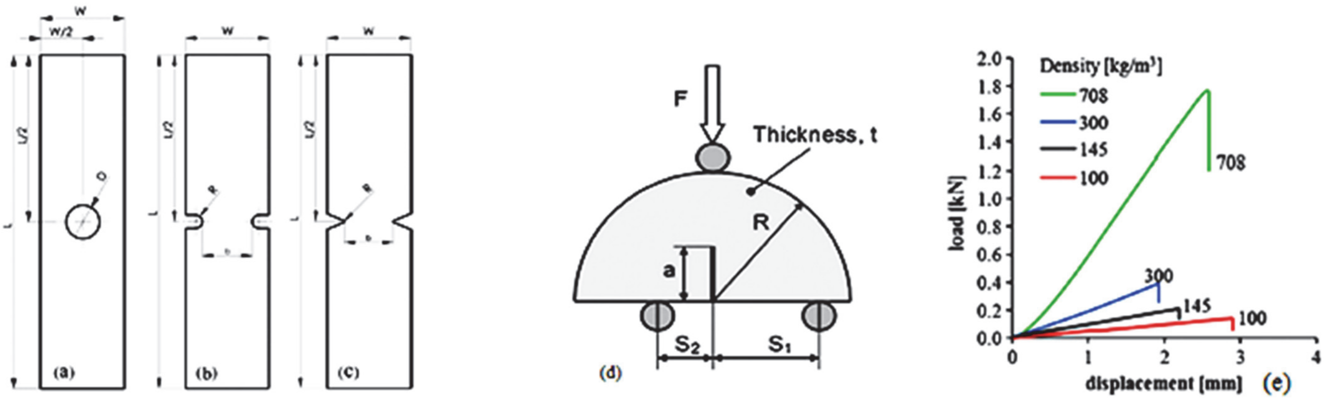

Figure 1: Notched specimens on tensile, (a) lateral rounded V notch, (b) lateral U notches, (c) circular hole and (d) ASCB specimen; (e) typical load-displacement curves on tensile and bending specimens.

THEORETICAL BACKGROUND

Berto and Lazzarin [27], and later Radaj and Vormwald [34], presented comprehensive overview of the volume-based strain energy density criterion. Below, only a reminder of the main concepts of the SED regarding brittle fracture of notched components is reviewed. SED criterion assumes that failure occurs when the mean value W of deformation energy in a local finite volume around the notch tip (control volume) reaches a critical value W_c; the failure occurs when $\bar{W} \geq W_c$, independent of the notch opening angle and loading type. If the material exhibits an ideally brittle behaviour until fracture, the parameter W_c is calculated from the ultimate tensile strength σ_u:

$$W_c = \sigma_u^2 / 2E \tag{2}$$

Under the situations when plain specimens exhibit a non-linear behaviour, whereas the notched specimens behave linear, Seweryn [35] recommended that the stress σ_u should be replaced by "the maximum normal stress existing at the edge at the moment preceding the cracking" determined on tensile specimens with blunt curvature radius, where semi-circular notches are recommended. In plane problems, the control volume becomes a circle or a circular sector with a radius R_c in the case of cracks or pointed V-notches in mode I or mixed, I + II, mode loading (Fig. 2a and b). Under plane strain conditions, a useful expression for R_c has been provided considering the crack case [36, 37]:

$$R_c = \frac{(1+v)(5-8v)}{4\pi}\left(\frac{K_{Ic}}{\sigma_t}\right)^2 \tag{3}$$

If the critical value of the NSIF is determined by means of specimens with $a \neq 0$, the critical radius can be estimated by means of the expression:

$$R_c = \left[\frac{I_1 \times K_{1c}^2}{4\lambda_1(\pi-\alpha)EW_c}\right]^{\frac{1}{(2-2\lambda_1)}} \tag{4}$$

When $2a = 0$, K_{1C} equals the fracture toughness K_{IC}. For rounded V-notches, a crescent-shaped control volume bounded by two radii differently centered was introduced: a circular notch edge with radius q as the inner boundary and a circle arc with radius $r_0 + R_c$ as the outer boundary, (Fig. 2c). The length r_0 represents the distance between the origin of the polar coordinates (used to express the stress field) and the notch tip. The parameters r_0 depends from q then it's function only from the geometry (the opening angle $2a$); r_0 is defined as $r_0 = qR/(q-1)$ where $q = (2\pi - 2\alpha)/\pi$.

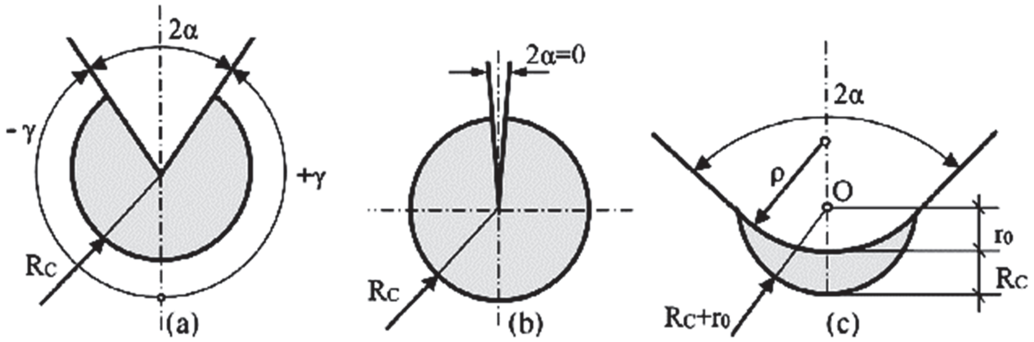

Figure 2: Control volume for sharp V notch (a), crack case (b) and rounded V notch under mode I loading.

The radius of the control volume and the critical strain energy density depend only from the mechanical properties of the material as the Young's Modulus, the fracture toughness, the Poisson's ratio and the ultimate tensile strength σ_u or σ_t.

NUMERICAL INVESTIGATIONS

Determination SED parameters

The quasi ideally brittle behavior, for these foams, is exhibited for notched components, Fig. 1e, so the ultimate tensile strength σ_u should be substituted with σ_t, the maximum normal tension presents at the notch tip in the moment that proceed the crack, tension calculated in a notched specimen under tensile load, specimen with a bland curvature radius. This σ_t can be evaluated using U notched specimen with a curvature radius greater than 4 mm, a bland notch: is recommended to use a semi-circular notches, in this paper it has been choose to use a plate with symmetric U notch. A linear-elastic finite element analysis was carried out in ANSYS 14.5 software for all specimen geometries. Based on symmetry of loading and boundary conditions quarter of geometry was considered. The average maximum load was applied to the models for each notch geometry as uniaxial loads. The PLANE184 plane 8-node bi-quadratic elements with a suitably high mesh density in the area of the notch tip were employed, the analysis are under plane strain conditions. According with the procedure described above, it's possible to define the tension at the notch tip. In Tab. 4 is exhibit the tension σ_t and the parameters of SED method, calculated through Eq. 2 and 3.

Density [Kg/m^3]	σ_t [MPa]	R_c [mm]	W_c [MJ/m^3]
100	3.19	0.20	0.169
145	4.39	0.24	0.143
300	6.06	1.0	0.065
708	26.7	0.62	0.285

Table 5: Values of tension at the notch tip and respective SED parameters.

Application SED method on specimens with different type of notch, mode I

Through the SED parameters determined previously, is possible to apply the SED method on the notched specimens tested in the previous paragraphs. In the same way followed to determine the σ_t tension, the SED method were applied through linear elastic finite element analysis, using plane elements (PLANE 184) and creating the control volume around the notch tip. The results are reported in Fig. 3.a. All the specimens are in mode I loads configuration. For the majority of the results, the scatter band is contained between + 10 % and – 22 %, a reasonable dispersion in engineering field.

Application SED method on specimens with different type of notch, mode I

ASCB specimens were tested under pure mode I, pure mode II and mixed mode I+II. The first approach is to use the SED parameters defined for mode I (Tab. 5) in the case of the mode II and mixed mode: for the higher densities, in mixed mode and in mode II the error is greater than 35 %, while for the lowest densities the error is contained between ± 10 %, Graph 1b. It has been noticed that the strain energy density increase from mode I to mode II. If it's possible to define the SED parameters, then the hypothesis that the material has a brittle behavior is valid and in the crack case (the control volume is a sector centered at the notch tip, Fig. 2.b) the strain energy density can be express through eq. (3).

$$W = \frac{e_1}{E}\frac{K_I^2}{R_c^{2(1-\lambda_1)}} + \frac{e_2}{E}\frac{K_{II}^2}{R_c^{2(1-\lambda_2)}} \quad (5)$$

The authors proposed the following approach: the control volume remains the same in all load configurations and it's equal to the control volume defined under pure mode I: in this way it's possible to recalculate the value of the critical strain energy density in mixed mode I+II and in pure mode II. Under this hypothesis, the scatter band is contained between ± 10 %, as it seen Fig. 3.c. In Fig. 3 the error is calculated using the W_c defined through the σ_t tension; the W_c can be redefined through the mean value of the strain energy density of each specimens. The new values of W_c are listed in Table 5: the errors using these values of critical energy density are presented in Fig. 4; except Necuron 301, the scatter band is contained between ± 15 %.

Density [Kg/m^3]	R_c [mm]	W_c [MJ/m^3]
100	0.20	0.140
145	0.24	0.111
300	1.0	0.039
708	0.62	0.21

Table 6: New values of critical energy density that fit better the results.

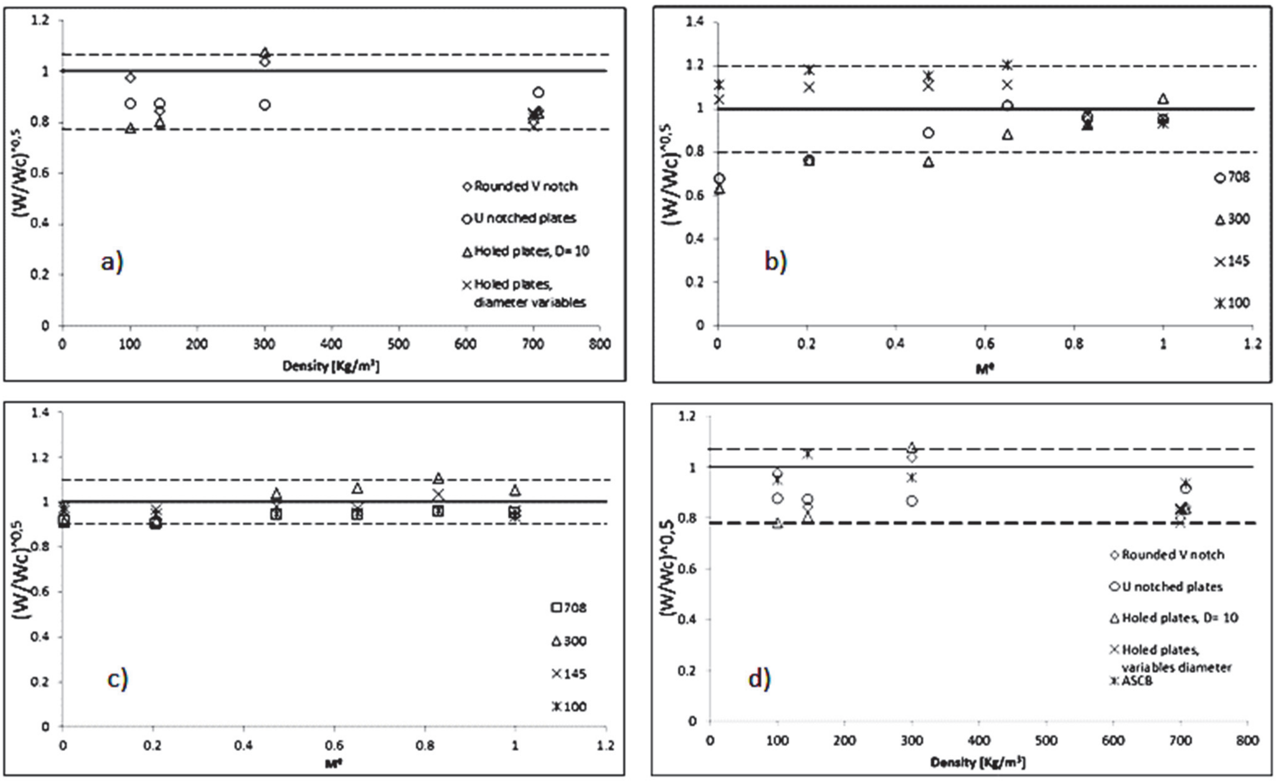

Figure 3: Ratio between the predictions of maximum loads and experimental loads: a) notched specimens, b) ASCB specimens under mixed mode, c) personal approach for ASCB specimens under mixed mode, d) all notched specimens under mode I.

Density [Kg/m^3]	σ_t [MPa]	$\sigma_{0,TCD}$ [MPa]
100	3.19	2.17
145	4.39	3.19
300	6.06	5.6
708	26.7	23.14

Table 7: Comparison between stress of TCD method and SED method.

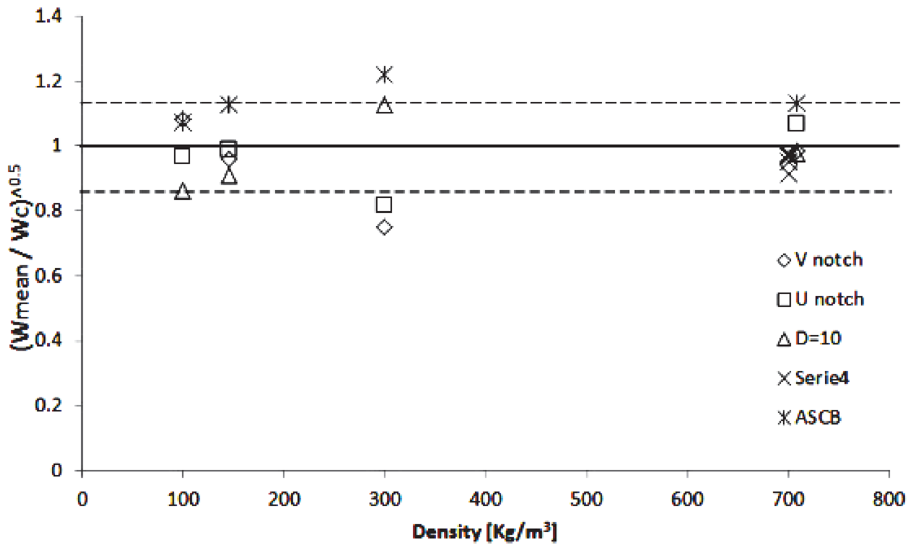

Figure 4: Ratio between the predictions of maximum loads and experimental loads using the new values of critical energy density.

CONCLUSIONS

Except some value, the relative errors is contained between +10 % and –22 %, a reasonable prediction in engineering field, Figs. 3 and 4. From these results it's possible to notice that the SED method works for these foams and the parameters (R_c and W_c) can be determined through experimental tests on tensile notched specimens. In a research by Negru et al. (2015) it's defined the inherent stress for the Theory of Critical Distance (TCD), an approach based on the same theory of SED method, they belong to the linear elastic mechanic fracture theory (LEFM). The inherent stress in TCD method is equivalent to the failure stress and this tension is defined in a different way: the stress σ_t defined in this paper is compared with the inherent stress of TCD method, Tab. 6. Two different approach give values of the tensions very similar, with the same order of magnitude, this confirms that it's possible to apply the SED method on these foams and the tensions σ_t that valid the SED for each type of notch have the same order of magnitude and it's similar.

The personal approach works but the hypothesis that the control volume remains the same it's only a personal view of the problem; this assumption it has been made only to prove that the PUR foams can be treated as a brittle materials and the SED approach can be applied, in fact the strain energy density defined through Eq. 3 differs less than ± 8% from the numerical strain energy density defined through the numerical investigations.

It's possible to define a new values of critical energy density for each density that permit to decrease the errors, in fact more than 95 % of the results are contained between ± 15 %, so the new values of W_c fit better the results. The paper represents an entry level approach for the determination of the SED parameters for these foams, it's necessary further studies and tests.

ACKNOWLEDGMENTS

The experimental results presented here were performed under the Grant of the Romanian National Authority for Scientific Research, CNCS-UEFISCDI, project PN-II-ID-PCE-2011-3-0456, contract number 172/2011. Mr. Alberto Piccotin was supported by ERASMUS program to carry on a research stage at University Politehnica Timisoara.

REFERENCES

[1] http://www.necumer.com/index.php/en/produkte-2/board-materials.html, (2014).
[2] Gibson, L.J., Ashby, M.F., Cellular Solids, Structure and Properties, second ed., Cambridge University Press, (1997).
[3] Ashby, M.F., Cellular solids – scaling of proprieties, in: M. Scheffler, P. Colombo (Eds.), Cellular Ceramics, Structure, Manufacturing, Properties and Applications, Wiley-VCH Verlag Gmbh & Co., (2005) 3–17.
[4] Marsavina, L., Fracture mechanics of cellular solids, in: H. Altenbach, A. Ochsner (Eds.), Cellular and Porous Materials in Structures and Processes, Springer, Wien, (2010) 1–46.
[5] Lazzarin, P., Comportamento a fatica dei giunti saldati in funzione della densità di energia di deformazione locale: influenza dei campi di tensione singolari e non singolari, Frattura ed Integrità Strutturale, 9 (2009) 13-26.
[6] Maragoni, L., Carraro, P. A., Peron, M. and Quaresimin, M., Fatigue behaviour of glass/epoxy laminates in the presence of voids, Int. J. Fatigue, 95 (2017) 18–28.
[7] Brotzu, A., Felli, F. and Pilone, D., Effects of the manufacturing process on fracture behaviour of cast TiAl intermetallic alloys, Frattura ed Integrità Strutturale, 27 (2013) 66-73.
[8] Ayatollahi, M.R., Razavi, S.M.J., Rashidi Moghaddam, M., Berto, F., Mode I fracture analysis of Polymethylmetacrylate using modified energy—based models. Phys. Mesomec., 18 (2015) 53-62.
[9] Ayatollahi, M.R., Rashidi Moghaddam, M., Razavi, S.M.J., Berto, F., Geometry effects on fracture trajectory of PMMA samples under pure mode-I loading. Eng. Fract. Mech., 163 (2016) 449–461.
[10] Ayatollahi, M.R., Razavi, S.M.J., Sommitsch, C., Moser, C., Fatigue life extension by crack repair using double stop-hole technique, Mater. Sci. Forum, 879 (2017) 3-8.
[11] Razavi, S.M.J., Ayatollahi, M.R., Sommitsch, C., Moser, C., Retardation of fatigue crack growth in high strength steel S690 using a modified stop-hole technique, Eng. Fract. Mech., 169 (2017) 226–237.
[12] Rashidi Moghaddam, M., Ayatollahi, M.R., Razavi, S.M.J., Berto, F., Mode II Brittle Fracture Assessment Using an Energy Based Criterion, Phys. Mesomec. (in press).
[13] Sih, G.C., Some basic problems in fracture mechanics and new concepts, Eng. Fract. Mech., 5 (1973) 365-377.
[14] Sih, G.C., Strain-energy-density factor applied to mixed mode crack problems, Int. J. Fracture, 10 (1974) 305-321.
[15] Kipp, M.E., Sih, G.C., The strain energy density failure criterion applied to notched elastic solids, Int. J. Solids Struct., 11 (1975) 153-173.
[16] Sih, G.C., Ho, J.W., Sharp notch fracture strength characterized by critical energy density, Theor. Appl. Fract. Mec., 16 (1991) 179-214.
[17] Lazzarin, P. and Zambardi, R., A finite-volume-energy based approach to predict the static and fatigue behavior of components with sharp V-shaped notches, Int. J. Fract., 112 (2001) 275–298.
[18] Berto, F., Lazzarin, P. and Ayatollahi, M. R., Brittle fracture of sharp and blunt V-notches in isostatic graphite under torsion loading, Carbon N. Y., 50 (2012) 1942–1952.
[19] Berto, F. and Barati, E., Fracture assessment of U-notches under three point bending by means of local energy density, Mater. Des., 32 (2011) 822–830.
[20] Radaj, D., Berto, F., and Lazzarin, P., Local fatigue strength parameters for welded joints based on strain energy density with inclusion of small-size notches, Eng. Fract. Mech., 76 (2009) 1109–1130.
[21] Lazzarin, P., Berto, F., Some expressions for the strain energy in a finite volume surrounding the root of blunt V-notches, Int. J. Fract., 135 (2005) 161-185.
[22] Gómez, F.J., Elices, M., Berto, F., Lazzarin, P., Local strain energy to assess the static failure of U-notches in plates under mixed mode loading, Int. J. Fract., 145 (2007) 29-45.
[23] Berto, F., Lazzarin, P., Gómez, F.J., Elices, M., Fracture assessment of U-notches under mixed mode loading: two procedures based on the 'equivalent local mode I' concept, Int. J. Fract., 148 (2007) 415-433.

[24] Lazzarin, P., Livieri, P., Berto, F. and Zappalorto, M., Local strain energy density and fatigue strength of welded joints under uniaxial and multiaxial loading, Eng. Fract. Mech., 75 (2008) 1875–1889.
[25] Lazzarin, P., Berto, F., Gómez, F.J., Zappalorto, M., Some advantages derived from the use of the strain energy density over a control volume in fatigue strength assessments of welded joints, Int. J. Fract., 30 (2008) 1345-1357.
[26] Lazzarin, P., Berto, F., Elices, M. and Gómez, J., Brittle failures from U- and V-notches in mode I and mixed, I + II, mode: A synthesis based on the strain energy density averaged on finite-size volumes, Fatigue Fract. Eng. M., 32 (2009) 671–684.
[27] Berto, F., Lazzarin, P., A review of the volume-based strain energy density approach applied to V-notches and welded structures, Theor. Appl. Fract. Mec., 52 (2009) 183-194.
[28] Marsavina, L., Constantinescu, D.M., Linul, E., Apostol, D.A., Voiconi, T., Sadowski, T., Refinements on fracture toughness of PUR foams, Eng. Fract. Mech., 129 (2014) 54–66.
[29] Marsavina, L., Constantinescu, D.M., Linul, E., Apostol, D.A., Voiconi, T., Sadowski, T., Evaluation of mixed mode fracture for PUR foams, Procedia Materials Science, 3 (2014) 1342–1352.
[30] Negru, R., Marsavina, L., Filipescu, H., Pasca, N., Investigation of mixed mode I/II brittle fracture using ASCB specimen, Int. J. Fracture, 18 (2013) 155–161.
[31] Ayatollahi, M.R., Torabi, A.R., 2009, A criterion for brittle fracture in U-notched components under mixed-mode loading, Eng. Fract. Mech., 76 (2009) 1883-1896.
[32] Lazzarin, P. and Filippi, S., A generalized stress intensity factor to be applied to rounded V-shaped notches. International J. Solids Struct., 43 (2006) 2461-2478.
[33] Ayatollahi, M.R., Torabi, A.R., A criterion for brittle fracture in U-notched components under mixed-mode loading. Eng. Fract. Mech., 76 (2009) 1883-1896.
[34] Radaj, D., Vormwald, M., Advanced Methods of Fatigue Assessment, Springer-Verlag, Berlin, (2013).
[35] Seweryn, A., Brittle fracture criterion for structures with sharp notches, Eng. Fract. Mech., 47 (1994) 673-681.
[36] Yosibash, Z., Bussiba, A., Gilad, I., Failure criteria for brittle elastic materials, Int. J. Fracture, 125 (2004) 307–333.
[37] Gallo, P., Berto, F., Glinka, G Generalized approach to estimation of strains and stresses at blunt V-notches under non-localized creep, Fatigue Fract. Eng. Mater. Struct., 39 (2016) 292-306.